Poly(*N*-vinylcaprolactam) Microgels and its Related Composites

Shufu Peng[1] and Chi Wu,[1,2,*]

1. Department of Chemistry, The Chinese University of Hong Kong, Shatin, Hong Kong
2. The Open Laboratory of Bond-selective Chemistry, Department of Chemical Physics, University of Science and Technology of China, Hefei, Anhui, China

SUMMARY: Spherical hydrogels were prepared by precipitation copolymerization of *N*-vinylcaprolactam and sodium acrylate [P(VCL-*co*-NaA)] at 60 °C. As a thermally sensitive polymer, the increase of temperature in the range 25–40 °C can lead to a continuous shrinking of PVCL homopolymer chains. The copolymerization of a few molar percent of NaA into a PVCL chain increases its swelling extent and shifts its shrinking temperature slightly higher. Our results revealed that in the shrinking process, calcium ions (Ca^{2+}) induced a profound complexation of the P(VCL-*co*-NaA) microgels at a critical temperature (T_c) which was nearly independent of the NaA content. However, both the rate and degree of the complexation increase as the NaA content increases at T_c. One the basis of this study, we further studied the complexation of P(VCL-*co*-NaA) microgels with gelatin in the presence of calcium ions and prepared chemically crosslinked of the gelatin gels with embedded P(VCL-*co*-NaA) microgels. Our results showed that the shrinking of the embedded P(VCL-*co*-NaA) microgels could lead to the shrinking of gelatin gels. The biomedical application of this gelatin/microgel composite have been exploited.

Introduction

Recently, swelling and shrinking of hydrogels under the different conditions, such as temperature, pH, composition, ionic strength and solvent, have attracted much attention. For example, hundreds of experimental and theoretical studies on thermally sensitive poly(*N*-isopropylacrylamide) (PNIPAM) gels have been reported[1)]. In general, a thermally sensitive hydrogel has a lower critical solution temperature (LCST); namely, it swells at lower temperatures but shrinks as the temperature increases. It is known that introducing a few molar percent of hydrophobic or hydrophilic groups into a hydrogel can alter its shrinking temperature and swelling extent[2)]. In contrast, reports on thermally sensitive microgels are much limited, partially because their preparation and observation are relatively more difficult. Experimentally, it is important to prepare microgels with a sufficient amount of crosslinking points so that each microgel is still a swollen three-dimensional polymer network. Using microgels offers several advantages. For example, microgels can nearly instantly reach their

 CCC 1022-1360/00/$ 17.50+.50/0

shrinking and swelling limits in comparison with days required by bulk gels. Microgels can also be injected in some special applications.

Poly(*N*-vinylcaprolactam) (PVCL) is a relatively new type of nonionic water-soluble polymer. It was developed for hair-care and cosmetic applications. In principle, it should be more biocompatible than PNIPAM. It has been known that PVCL can complex with organic compounds[3], resist hydrolysis, and its gel can undergo a continuous volume transition in the temperature range 25–36 °C[4]. Up to now, only a few studies on PVCL and its gels have been reported partially because its polymerization is more difficult and partially because its volume transition is not as sharp as that of the PNIPAM gels. However, its biocompability attracts us to initiate this study to see whether PVCL microgels can be used as an injecting composition for certain biomedical applications. It is also known that a certain kind of metal ions, such as Ca^{2+}, can interact with carboxylic groups on polymer chains via a polyion/metal complexation to form interchain aggregation[5]. This complexation led us to think whether it can be used to immobilize microgels incorporated with a proper amount of carboxylic groups inside body after injection. This study is a fundamental research with some envisioned biomedical applications.

Experimental

Materials. *N*-vinylcaprolactam monomer (VCL, courtesy of BASF) was further purified by a reduced pressure distillation. Sodium acrylate monomer (NaA, from Lancaster) was used without further purification. Potassium persulfate as an initiator (KPS, from Aldrich) and *N*',*N*'–methylenebisacrylamide as a cross-linking agent (MBAA, from Aldrich) were recrystallized three times in methanol. The gelatin sample (courtesy of BASF) had a weight average molar mass of 1.5×10^5. To have a complete dissolution of gelatin, 2% of formamide was added into water to break interchain hydrogen bonding. Calcium chloride (anhydrous $CaCl_2$, from ACROS) was used without further purification.

Microgel preparation. Spherical poly(*N*-vinylcaprolactam-*co*-sodium acrylate) [P(VCL-*co*-NaA)] microgels were prepared by precipitation polymerization in water. Into a 150-mL three-neck flask equipped with a reflux condenser, a thermometer and a nitrogen-bubbling tube, were added 7.3 mmol VCL monomer, a proper amount of NaA comonomer, 0.19 mmol MBAA, and 40 mL deionized water. The solution was stirred and bubbled by nitrogen for 1 hr to remove oxygen before 0.045 mmol KPS aqueous solution was added to start the

polymerization at 60 °C for 24 hrs. The resultant P(VCL-*co*-NaA) microgels were purified by a successive four times centrifugation (Sigma 2K15 ultracentrifuge, at 15,300 rpm and 40 °C), decantation and redispersion in deionized water to remove unreacted low molar mass molecules. Such obtained P(VCL-*co*-NaA) microgels were diluted with deionized water to concentrations lower than ~1 × 10^{-5} g/mL in laser light scattering measurements. The microgels with different contents of NaA were labeled as P(VCL–*m*A), where "*m*" represents the average molar content of acrylic groups. Linear P(VCL-*co*-NaA) chains was prepared in a similar way without adding the crosslinking agent, MBAA.

Laser light scattering (LLS). The detail of our laser light scattering spectrometer can be found elsewhere[6]. In static LLS, the angular dependence of the absolute excess time-averaged scattered intensity, known as the Rayleigh ratio $R_{vv}(q)$, can lead to the weight-average molar mass (M_w), the z-average root-mean-square radius of gyration ($\langle R_g^2 \rangle_z^{1/2}$, or written as $\langle R_g \rangle$) and the second virial coefficient (A_2), where q is the scattering vector. In dynamic LLS, the cumulant or Laplace inversion analysis of the measured intensity-intensity time correlation function $G^{(2)}(q,t)$ in the self-beating mode can result in an average line width ($\langle \Gamma \rangle$) or a line width distribution ($G(\Gamma)$)[7]. For a pure diffusive relaxation, Γ is related to the translational diffusion coefficient D by $(\Gamma/q^2)_{C\to 0, q\to 0} = D$ and to the hydrodynamic radius (R_h) by the Stokes-Einstein equation, $D = k_B T/(6\pi\eta R_h)$, where k_B, T and η are the Boltzmann constant, the absolute temperature and the solvent viscosity, respectively[8].

Results and discussion

Table 1 summarizes static and dynamic LLS results of spherical microgels with different contents of NaA in the absence of Ca^{2+} in the swollen (27 °C) and collapsed (50 °C) states. In each case, M_w is independent of the temperature, indicating no interchain or no interparticle aggregation. On the other hand, the shrinking of the microgels as the temperature increases was relatively smooth, similar to the temperature-induced volume change of neutral PVCL microgels[4]. However, the ionic groups make the PVCL chain more hydrophilic, which leads to a higher swelling extent at lower temperatures, shifts the shrinking temperature higher, and results in a less compact globule[9]. The increase of the ratio of average gyration radius to average hydrodynamic radius ($\langle R_g \rangle / \langle R_h \rangle$) as the ionic content increases indicates further swelling of the microgels.

Figure 1 clearly shows the temperature dependence of the relative average hydrodynamic radius $\langle R_h \rangle / \langle R_h \rangle_{T=25°C}$ for P(VCL-*co*-NaA) microgels copolymerized with different amounts of NaA, where $\langle R_h \rangle_{T=25°C}$ is the average hydrodynamic radius $\langle R_h \rangle$ at 25° C. The relative shrinking of the microgels decreases as the ionic content increases. Note that in the temperature range studied, there was no change in M_w in each case, i.e., no inter-microgel aggregation in the shrinking process.

Table 1. Light scattering characterization of spherical P(VCL-*co*-NaA) microgels in water.

	P(VCL-*1.0*NaA)			P(VCL-*9.1*NaA)		
T / °C	$M_w \times 10^9$ / g/mol	$\langle R_h \rangle$ / nm	$\langle R_g \rangle / \langle R_h \rangle$	$M_w \times 10^9$ / g/mol	$\langle R_h \rangle$ / nm	$\langle R_g \rangle / \langle R_h \rangle$
27	1.34	330	0.70	5.54	515	1.29
37	1.40	191	0.73	5.41	371	0.91
50	1.42	134	0.85	5.21	272	1.11

Figure 2 shows a better view of the shrinkings of microgels in terms of the average chain density ($\langle \rho \rangle$) defined as $M_w/((4/3)\pi\langle R_h \rangle^3)$. P(VCL-*1.0*NaA) microgels reached their corresponding collapsed states at 42 °C. The slow increase of $\langle \rho \rangle$ for the P(VCL-*9.1*NaA) microgels can be attributed to a balance between strong electrostatic repulsion and hydrophobic attraction. If using $\langle \rho \rangle$ at 25 °C as a reference, we found that $\langle \rho \rangle$ increases 8–16 times for the microgels, depending on the ionic content for the P(VCL-*1.0*NaA) microgels.

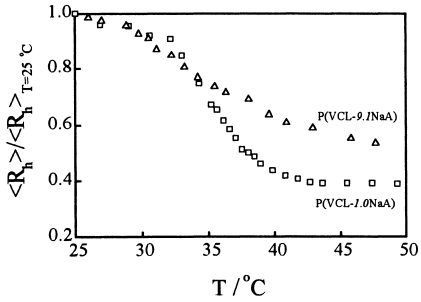

Fig. 1: Temperature dependence of the relativ average hydrodynamic radius $\langle R_h \rangle / \langle R_h \rangle_{T=25°}$ for P(VCL-*co*-NaA) microgels with differen amounts of NaA, where $\langle R_h \rangle_{T=25°C}$ is th average hydrodynamic radius $\langle R_h \rangle$ at 25° C.

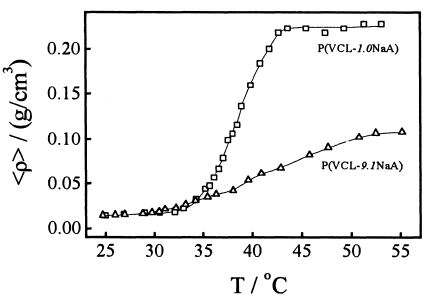

Fig. 2: Temperature dependence of the average chain density $\langle \rho \rangle$ of P(VCL-*co*-NaA) microgels with different amounts of NaA.

Figures 3 and 4 show a complete different picture of the temperature dependence of the average hydrodynamic radius ($<R_h>$) and the apparent weight average molar mass ($M_{w,app}$) of microgels in a 0.03M $CaCl_2$ aqueous solution. In the range 25–31.8 °C, the microgel shrinks as the temperature increases, but $M_{w,app}$ is independent of the temperature, indicating no inter-microgel aggregation. At ~32 °C, the average hydrodynamic size and the apparent weight average molar mass sharply increases, revealing a clear inter-microgel aggregation. The aggregation number of the microgels (N_{agg}) varies from 40 to 200 as the ionic content increase. This is understandable because for the microgels, when the temperature reaches the transition temperature, PVCL becomes hydrophobic and starts to collapse, but the hydrophilic $-COO^-$ groups tend to stay on the periphery of the microgel. The complexation between Ca^{2+} ions and $-COO^-$ sticks the microgels together and the complexation occurred in a narrow temperature range. Our results showed that the resultant complexes have a similar average chain density $<\rho>$ of ~0.2 g/cm^3, in spite of a big different in N_{agg}. A slight decrease of $<\rho>$ as the ionic content increases can be attributed to the fact that the chains with more ionic groups are more hydrophilic and collapse less at high temperatures. Note that microgels have a amphiphilic character at higher temperatures. The shrinking of each linear chain forces most of the ionic groups to form a relatively more hydrophilic periphery, similar to a micelle[10], while in the case of the microgels, most of the ionic groups are trapped inside the microgel due to the crosslinking, so that there are less chances to form the inter-microgel complexes, which explains why N_{agg} (microgel) decreases as the ionic content increases.

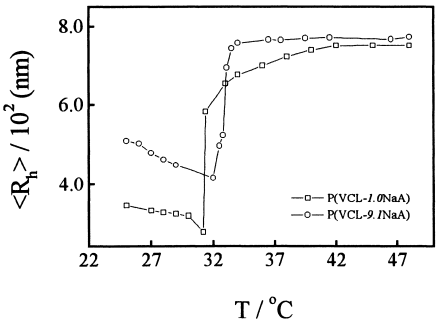

Fig. 3: Temperature dependence of the average hydrodynamic radius $<R_h>$ of spherical P(VCL-*co*-NaA) microgels in the presence of Ca^{2+}.

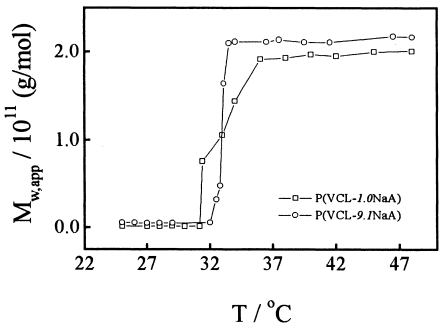

Fig. 4: Temperature dependence of the and the apparent weight average molar mass ($M_{w,app}$) of spherical P(VCL-*co*-NaA) microgels in the presence of Ca^{2+}.

Figures 5 and 6 show the temperature dependence of $<R_h>$ and $M_{w,app}$ for P(VCL-*4.3*NaA) microgels in the presence of different amounts of Ca^{2+}. Note that the complexation occurs at a similar temperature in spite of different Ca^{2+} concentrations, but both $<R_h>$ and $M_{w,app}$ increase as $[Ca^{2+}]$ increases. The increase of the ionic content has little effect on $<R_h>$. Our results reveal that the average number of the microgels inside each inter-microgel complex (N_{agg}) are ~60, ~20 and ~8 for $[Ca^{2+}] = 3 \times 10^{-2}$ M, 2×10^{-3} M and 2×10^{-4} M, respectively. The average chain density $<\rho>$ of the complexes decreases as N_{agg} decreases, which could be due to an imperfect packing of larger microgels inside each complexes, especially when each complex is only made of ~8 microgels.

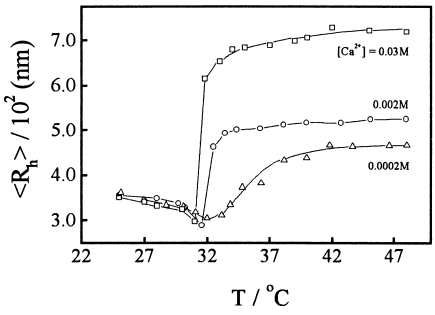

Fig. 5: Temperature dependence of the average hydrodynamic radius $<R_h>$ of P(VCL-*4.3*NaA) microgels with different Ca^{2+} concentrations.

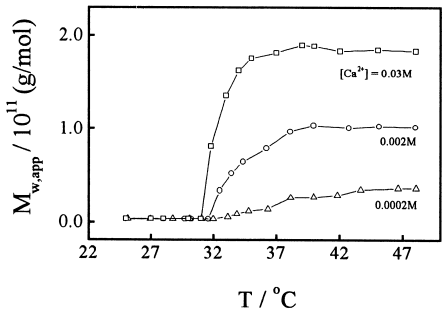

Fig. 6: Temperature dependence of apparent weight average molar mass ($M_{w,app}$) of P(VCL-*4.3*NaA) microgels with different Ca^{2+} concentrations.

Figure 7 shows that temperature dependence of $<R_h>$ and $M_{w,app}$ of the P(VCL-*4.3*NaA)/gelatin mixtures with different gelatin/P(VCL-*4.3*NaA) ratios (C_g/C_p), where C_g and C_p are the average weight concentrations of gelatin and microgels, respectively. At T ~32 °C, both $<R_h>$ and $M_{w,app}$ of the mixtures slightly increase, revealing the mixtures undergo an association between the microgels and gelatin. A further increasing of the temperature led to a gradual decrease of $<R_h>$, but $M_{w,app}$ is independent of the temperature in the same range, indicating no further association. For the mixture with a lower ratio C_g/C_p, $<R_h>$ decreases smoothly as the temperature increases in the whole range studied. The results in Figure 7 indicates that the shrinking of the P(VCL-*co*-NaA) microgels could lead to the shrinking of the gelatin/microgel complexes. More P(VCL-*co*-NaA) microgels inside the complexes provide a larger shrinking force and a more compact final structure.

Figure 8 shows that the temperature dependence of $<R_h>$ and $M_{w,app}$ of P(VCL-*4.3*NaA)/gelatin mixtures in the presence of Ca^{2+}. Note that the complexation occurs at a similar temperature in spite of a difference in the gelatin concentration. The complexation in the presence of Ca^{2+} is much profound than in Figure 7. Both $<R_h>$ and $M_{w,app}$ increase as the C_g/C_p ratio decreases, indicating that gelatin acts as a stabilizer, presumably via an adsorption of gelatin chains on the microgels surface.

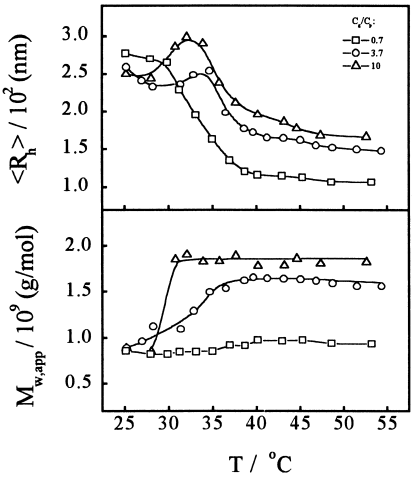

Fig. 7: Temperature dependence of the average hydrodynamic radius $<R_h>$ and apparent average molar mass weight average molar mass ($M_{w,app}$) of P(VCL-*4.3*NaA)/gelatin mixtures.

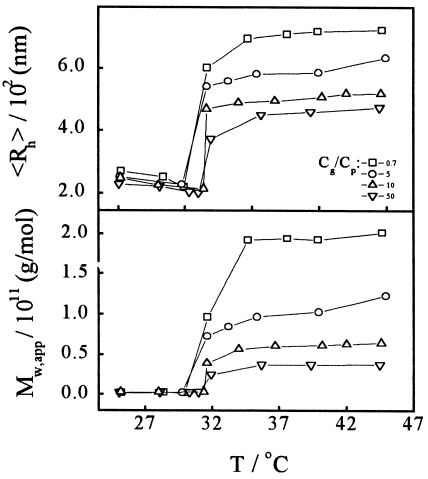

Fig. 8: Temperature dependence of the average hydrodynamic radius $<R_h>$ and the apparent weight average molar mass ($M_{w,app}$) of P(VCL-*4.3*NaA)/gelatin mixtures in the presence of Ca^{2+}.

Figure 9 shows that a bulk gel composite in which the microgels are embedded inside a chemically crosslinked gelatin network. It clearly shows that the shrinking of the microgels leads to a shrinking of the bulk gel composite. The degree of the shrinking can be controlled by the amount of the microgels embedded inside the gelatin network and by the crosslinking density. Such a gelatin/microgel composite is a potential biomedical material.

Figure 10 shows an *in vivo* biocompatibity test. The gel composite was inserted into a rat body at a sciatic never. The shrinking of a gel tube can connect a broken sciatic never at 37 °C. Note that the sciatic never has recovered after 20 weeks and the gel was completely absorbed by body.

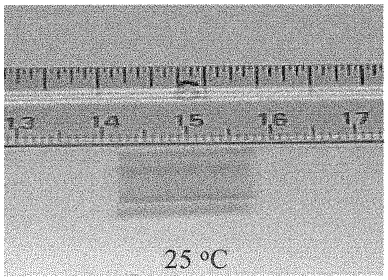

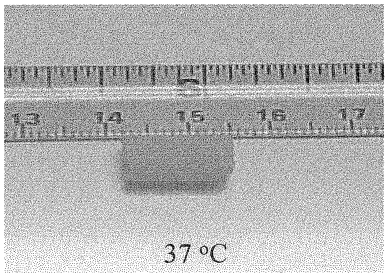

Fig. 9: Swelling and shrinking of the PVCL/gelatin composite at the different temperatures.

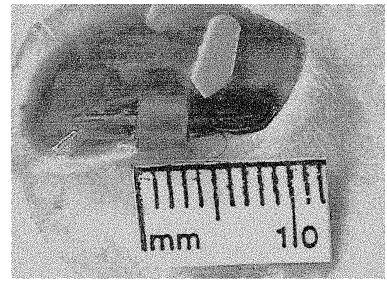

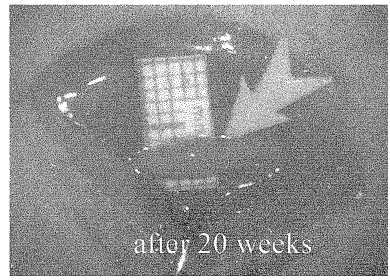

Fig. 10: Sciatic never before and after embedded the PVCL/gelatin gel tube into rat body.

References

1. S. Sat, M. Kong, H. Inmate, *Adv. Polym. Sci.* **109,** 207 (1993).
2. S. Zhou, B. Chu, *J. Phys. Chem. B* **102**, 1364 (1998).
3. M. Eisele, W. Burchard, *Makromol. Chem.* **191**, 169 (1991).
4. L. M. Mikheeva, N. V. Grinberg, A. Ya. Mashkevich, V. Ya. Grinberg, *Macromolecules* **30**, 2693 (1997).
5. S. Peng, C. Wu, *Macromolecules* **32**, 585 (1999).
6. X. Wang, Z. Xu, Y. Wan, T. Huang, S. Pispas, J. W. Mays, C. Wu, *Macromolecules* **30,** 7202 (1997).
7. B. Chu, *Laser Light Scattering, 2nd Ed.*; Academic Press, New York 1991.
8. W. H. Stockmayer, M. Schmidit, *Pure Appl. Chem.* **54**, 407 (1982).
9. K. Otake, H. Inomata, M. Konno, S. Saito, *J. Chem. Phys.* **91**, 1345 (1989).
10. M. Annaka, T. Tanaka, *Nature* **355**, 430 (1992).